Analytical Model for Pullout of Soil Reinforcement

ZEHONG YUAN AND KOON MENG CHUA

A closed-form solution for describing the pullout behavior of reinforcements embedded in soils is presented. The solution shows that pullout resistance is an explicit function of pullout displacement, reinforcement axial stiffness, interface shear stiffness, and reinforcement length. Laboratory pullout box tests as well as uniaxial tension tests were performed to obtain these parameters. The laboratory results of pullout versus displacement of a geogrid and a geotextile in sand are compared with the assumptions found in the current state of the practice. An example problem involving a geotextile and a geogrid in sand is used to illustrate the interaction among the four variables. The analytical solution shows that the shear stress is not uniform along the length of the reinforcement. The effective reinforcement length at which tension is nonzero is shown to vary with the two stiffness values as well as with the magnitude of the pullout force. Practical applications of this new analytical model are proposed.

The maximum force required to cause a pullout of reinforcement from a soil mass is of major concern to engineers designing reinforced earth structures. These reinforcements may be in the form of galvinized steel strips or geosynthetics such as geogrids or geotextiles. One of the more popular methods for determining pullout resistance and soil-reinforcement interactions properties is the pullout box method. The pullout box test essentially consists of pulling a piece of reinforcement through a slit or gap, away from the soil mass in which it is embedded. The applied force and the corresponding displacement are measured during the test. The pullout force is usually expressed in terms of per unit width of reinforcing material and is commonly referred to as the "pullout resistance." The apparent shear stress is calculated by dividing the pullout resistance by twice the plan area of the embedded reinforcement.

At present, laboratory test results obtained from the pullout box and the direct shear box are interpreted in the manner just described, that is, assuming a uniform shear stress distribution over the exposed area of the embedded reinforcement material (*1–6*). As such, the apparent soil-reinforcement interaction properties are based on an average stress. In reality, the shear stress distribution is not uniform, and it is obvious that the stress will approach zero at some distance from the pullout end if the embedded reinforcement is long enough. In other words, for that applied force magnitude, there will be an "effective" reinforcement length beyond which it is redundant. To date, little attention has been given to describing this stress distribution profile. This paper presents an analytical solution that explicitly relates the pullout resistance as a function of pullout displacement, soil-reinforcement interface properties, reinforcement stiffness, and reinforcement length.

This theoretical relationship will be shown to be very helpful in understanding the pullout phenomenon, in interpreting experimental pullout test results, and in improving the accuracy of design methods.

Department of Civil Engineering, University of New Mexico, Albuquerque, N.Mex., 87131.

DESIGNING REINFORCED EARTH STRUCTURES: CURRENT PRACTICE

Soil reinforcement essentially involves introducing elements that can take tension into the soil mass and as a result increase the stability of the earth structure. This concept was first recognized by Henri Vidal in the 1950s. In his investigation he concluded that when a dry granular soil is combined with a rough flexible material having tensile strength, the resulting "reinforced earth" is stronger than soil alone (*7*).

Reinforced earth technology has found wide application in geotechnical engineering in the past decade. Reinforced earth walls and reinforced slopes are examples of these applications. Figure 1 shows the components in a typical reinforced earth structure, in this case a reinforced earth wall. The reinforcement layers are usually embedded some distance away from the slope face or the front facing, if any.

Typical Design Approach

The conventional method for analyzing and designing these types of structures is by using the limit equilibrium approach. Basically, the steps involved are

1. Assume a failure surface,
2. Check equilibrium of the reinforced soil mass above that surface and calculate the safety factor, and
3. Repeat Steps 1 and 2 until a minimum safety factor is found.

Referring again to Figure 1, the potential failure surface refers to the surface intersecting the different reinforcement layers at their respective points of maximum tensile force. The maximum tensile force line separates two zones, namely, an active zone behind the wall facing where the shear stresses from the soil are directed outward, causing the reinforcements to be in tension, and a resistant zone where shear stresses are mobilized from the soil to resist the slipping of the reinforcements.

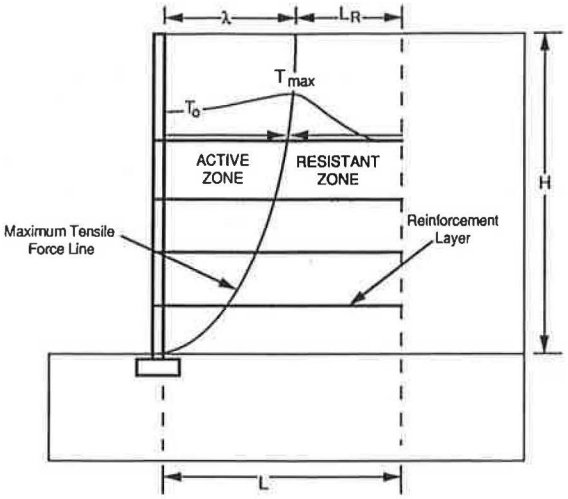

FIGURE 1 Design considerations in typical reinforced earth structure.

In most practical design procedures, Step 3, which involves assuming new failure surfaces, is not performed because the maximum tensile force line can be reasonably estimated. According to Schlosser et al. (*1*), the location of the line may be conservatively approximated in the following manner: at the upper part of the wall, the maximum tensile force is located along a vertical line at a distance (λ) of one-third of the wall height (H) from the wall facing. At the lower part of the wall, the maximum tension force is located on a line that is inclined at an angle of 45 degrees to the horizontal and that passes through the toe of the wall.

Determining Required Reinforcement Length

The total length (L) of each reinforcing layer is divided into two parts, namely, the active length (λ) and the resistant length (L_R). The reinforcement at each level of the earth structure must be of an adequate length to resist the pullout force anticipated at that level. This can be calculated by

$$L_R = \frac{T_m}{2b\, f^*\, \sigma_n} \tag{1}$$

where

b = width of reinforcement,
f^* = apparent coefficient of friction (value 0–1),
σ_n = overburden pressure, and
T_m = maximum tensile force in reinforcement.

Additionally, Schlosser et al. (*1*) suggested that the reinforcement length should be adequate to provide a factor of safety of 1.5 or greater with respect to the anticipated maximum pullout force or

$$\frac{L - \lambda}{L_R} \geq 1.5 \tag{2}$$

Substituting Equation 1 into Equation 2 yields

$$L \geq 1.5\left(\frac{T_m}{2bf^*\,\sigma_n}\right) + \lambda \tag{3}$$

Equation 3 is used to calculate the total length of the reinforcement at each reinforcement level.

Determining Apparent Friction Coefficient

The apparent friction coefficient (f^*) is an interaction property that is dependent on the type of reinforcement and the soil properties. Thus, to be accurate, it should be obtained by laboratory testing using the proposed reinforcement and the soil under the expected field conditions from the project site.

DEVELOPING NEW PULLOUT EQUATION

The following sections show the development of the closed-form solution describing the pullout behavior of reinforcements.

Figure 2 shows the schematic diagram of a pullout of a reinforcement at the point of maximum tensile force. The interface shear stress at Point x distance along the x-axis is related to the tensile force in the reinforcement at that point by

$$\tau(x) = \frac{1}{2}\left[\frac{\partial T(x)}{\partial x}\right] \tag{4}$$

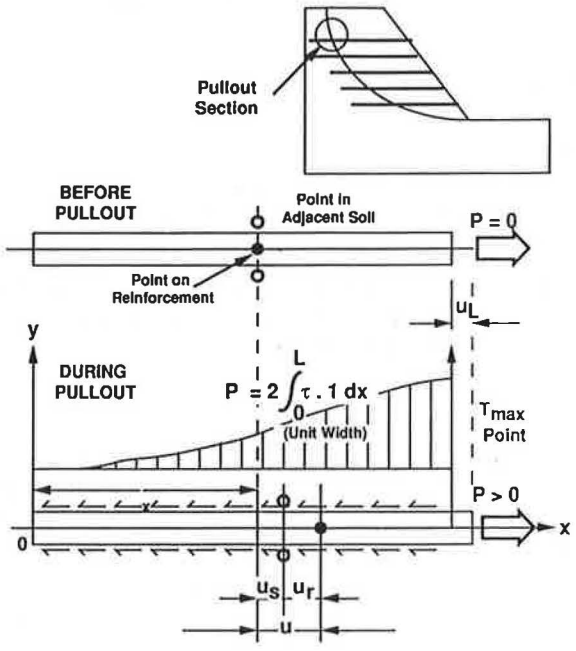

FIGURE 2 Relative displacement between soil and reinforcement.

where

x = longitudinal coordinate,
$\tau(x)$ = interface shear stress at x, and
$T(x)$ = tensile force at x in the reinforcement.

In addition, $T(x)$ is also related to tensile strain in the reinforcement in the following manner:

$$T(x) = k_a \varepsilon(x) = k_a \frac{\partial u(x)}{\partial x} \quad (5)$$

where

k_a = reinforcement stiffness,
$\varepsilon(x)$ = tensile strain of reinforcement at x, and
$u(x)$ = displacement of reinforcement at x.

The shear stress is related to the relative shear displacement and described by the following equation:

$$\tau(x) = k_s u_r \quad (6)$$

where k_s is the interface shear stiffness and u_r is the relative shear displacement. The relative shear displacement is the difference between displacement of a point in the reinforcement and a point in the adjacent soil mass as a result of pullout. These two points in the original configuration should have the same x-coordinates and a very small difference in the y-coordinates. The shear displacement (u_r) can be then expressed as

$$u_r(x) = u(x) - u_s(x) \quad (7)$$

where u_s is the displacement in soil adjacent to reinforcement in the x-direction, as illustrated in Figure 2. Following the definition of engineering strain, the shear strain developed in soils adjacent to the reinforcement can be defined as

$$\gamma_s = \frac{\partial u_s}{\partial y} + \frac{\partial v_s}{\partial x} \quad (8)$$

where

γ_s = engineering shear strain of soil,
v_s = vertical displacement of the adjacent soil, and
y = vertical coordinate.

The compatibility of interface shear stress requires that the shear stress acting on reinforcement and in the adjacent soil to be equal in magnitude, that is,

$$k_s u_r = G_s \gamma_s \quad (9)$$

where G_s is the shear modulus of the adjacent soil. Substituting Equations 5 and 6 into Equation 4 and Equation 9 into Equation 8 yields the following governing equations describing the pullout phenomenon of a reinforcement in soil:

$$k_a \frac{\partial^2 u}{\partial x^2} = 2k_s u_r \quad (10)$$

$$k_s u_r = G_s \left(\frac{\partial u_s}{\partial y} + \frac{\partial v_s}{\partial x} \right) \quad (11)$$

SOLVING GOVERNING EQUATIONS

To solve the previous two simultaneous partial differential equations analytically, it is necessary to assume that the soil displacement (u_s) is very small in comparison with the reinforcement displacement (u). In other words, shear strain is allowed and translation of the adjacent soil element is not. As a result, Equation 7 can be reduced to

$$u_r(x) = u(x) \quad (12)$$

The pullout phenomenon can now be described by one differential equation:

$$k_a \frac{\partial^2 u}{\partial x^2} = 2\, k_s u \quad (13)$$

The boundary conditions associated with Equation 13 are as follows:

$$T(0) = k_a \left(\frac{\partial u}{\partial x} \right)_{x=0} = 0 \quad (14)$$

$$T(L) = k_a \left(\frac{\partial u}{\partial x} \right)_{x=L} = P \quad (15)$$

where P is the applied pullout force per unit width of the reinforcement. The general solution to Equation 13 for displacement u is

$$u = C_1 e^{\alpha x} + C_2 e^{-\alpha x} \quad (16)$$

and

$$\alpha = \sqrt{\frac{2k_s}{k_a}} \quad (17)$$

Using the boundary conditions from Equations 14 and 15, C_1 and C_2 are found to be

$$C_1 = C_2 = \frac{P}{\alpha k_a (e^{\alpha L} - e^{-\alpha L})} \quad (18)$$

Substituting Equation 18 into Equation 16 yields the following:

$$u = \frac{P}{\alpha k_a (e^{\alpha L} - e^{-\alpha L})} (e^{\alpha x} + e^{-\alpha x}) \quad (19)$$

or

$$u = \frac{P \cosh(\alpha x)}{\sqrt{2k_a k_s} \sinh(\alpha L)} \quad (20)$$

From Equations 5 and 20, the distribution of tensile force along a reinforcement is

$$T = \frac{P \sinh(\alpha x)}{\sinh(\alpha L)} \quad (21)$$

From Equations 4 and 20, the distribution of interface shear stress is

$$\tau = \frac{1}{2} P\alpha \frac{\cosh(\alpha x)}{\sinh(\alpha L)} \tag{22}$$

Because the pullout response is usually described by the relationship of the applied pullout force (P) versus the pullout displacement (u) measured at the end where the force is applied, Equation 20 can be rewritten as

$$P = \sqrt{2k_s k_a} \tanh(\alpha L)\, u \tag{23}$$

Equations 20, 21, 22, and 23 are exact if the assumption that the soil displacement (u_s) is negligible when compared with the reinforcement displacement (u) is accurate. This assumption is acceptable because the soil will only move when the soil reinforcement system becomes globally unstable.

DETERMINING STIFFNESS PARAMETERS IN LABORATORY

To show the relationships between parameters in the new solution, pullout tests were performed for a geotextile (Geolon 200) and a geogrid (Tensar UX1100) in a fine, well-graded sand. The unit weight of the sand is 108 pcf and the relative density is about 70 percent. Results from conventional triaxial tests indicate the angle of internal resistance of 42 degrees.

Pullout Box Test

The pullout box at the University of New Mexico was designed and built in 1985 for the New Mexico State Highway and Transportation Department (NMSHTD) and is described in detail by Carney (*8*). The internal dimensions of the steel box are 30 in. long, 28 in. wide, and 24 in. deep. The loading system consists of three 20-ton-capacity hydraulic jacks, one of which is used to apply the vertical load and the others for the pullout. Strain-gage type load cells are used to measure applied loads. The applied vertical load is transmitted to the soil by an assemblage of thick wooden blocks, and it is assumed to be uniformly distributed in the soil mass before the pullout force is applied. The reinforcement is usually pulled at a constant rate after the vertical pressure is applied and the pullout distance is measured by linear variable differential transducers (LVDTs).

Axial Stiffness

The axial stiffnesses of a geogrid and a geotextile were obtained by uniaxial tension tests (without soil). The specimens were 48 in. long and 18 in. wide. Figure 3 shows the relationship of the tensile force and the strain of the two specimens, respectively. Figure 4 shows the axial stiffness of the specimens. The axial stiffness, or the membrane stiffness, is measured in pounds per inch and refers to the slope of the tensile force versus strain curve. Referring again to Figure 3, because the specimens are 48 in. long, a 1 percent strain will

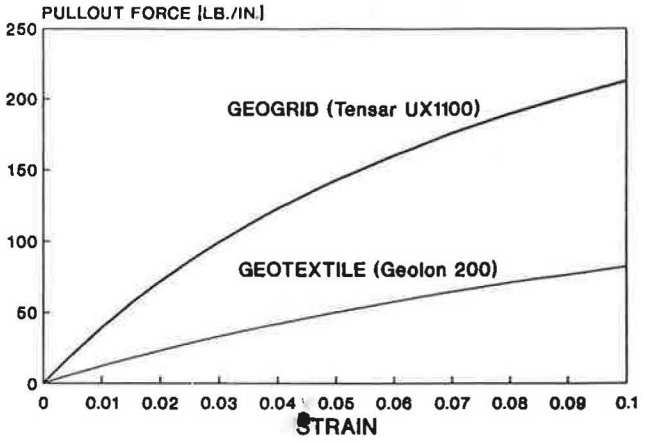

FIGURE 3 Results of uniaxial tension test with geotextile and geogrid for specimen 48 in. long.

be about ½ in. of displacement. At this displacement, it can be seen from Figure 4 that the axial stiffnesses of the Geolon 200 and Tensar UX1100 are reduced by about 10 and 20 percent, respectively. However, in practice this amount of extension over the entire length will not occur because much of the load is transferred to the soil.

Shear Stiffness

Figures 5 and 6 show the plots of pullout force versus displacement for Geolon 200 and Tensar UX1100 in sand, respectively. The pullout force (in pounds per inch width) is for a 30-in.-long reinforcing member that is in contact with the soil.

Yuan and Chua (*9*) argued that it is incorrect to assume that the shear stress is simply the pullout force divided by the area of reinforcing element in contact with the soil. This is because first, the shear stress distribution is not uniform, and second, the entire length of the embedded reinforcement need not be effective, as will be shown in the last section. It was proposed that the shear stress can be described as

$$\tau = \frac{u}{a + bu} \tag{24}$$

and the shear stiffness is obtained as

$$k_s = \frac{a}{(a + bu)^2} \tag{25}$$

where a and b are values dependent only on the applied vertical pressure for that particular interface and u is the pullout displacement at that point on the interface.

The shear stiffness curves shown in Figures 7 and 8 were obtained by trial and error using a finite element program called GEOT2D that was developed by the authors. GEOT2D (Geotechnical Engineering Two-Dimensional Analysis) uses nonlinear soil properties in simulating the continuum elements, and it also uses nonlinear interface elements and membrane elements to model the reinforced earth structure. Large deformation is allowed through the updated Lagrangian for-

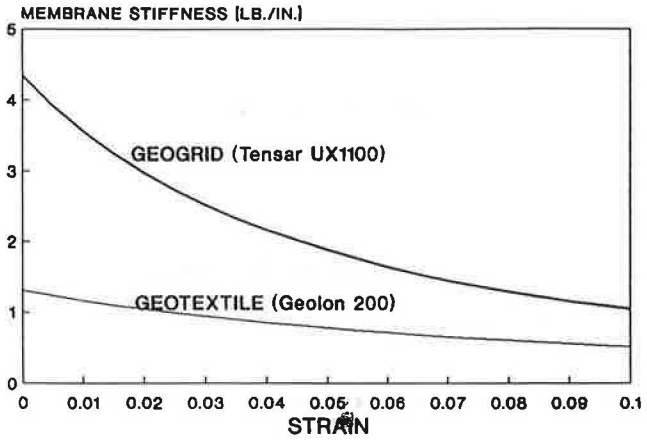

FIGURE 4 Axial stiffnesses of geotextile and geogrid for specimen 48 in. long.

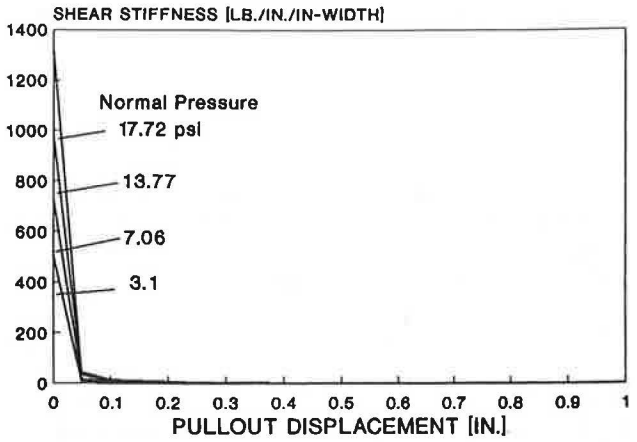

FIGURE 7 Interpreted shear stiffness of geotextile (Geolon 200) in sand.

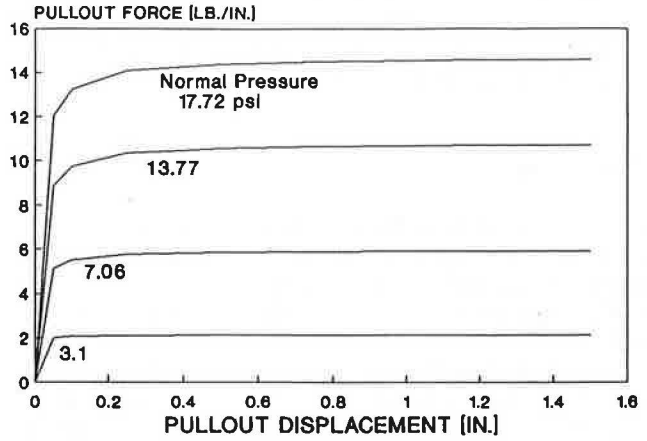

FIGURE 5 Results of pullout box test with geotextile (Geolon 200) in sand.

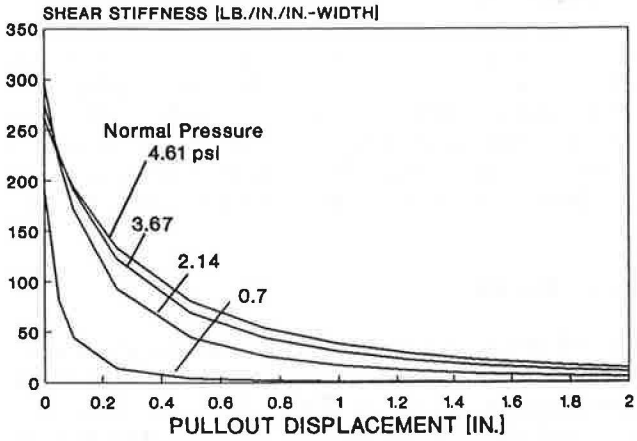

FIGURE 8 Interpreted shear stiffness of geogrid (Tensar UX1100) in sand.

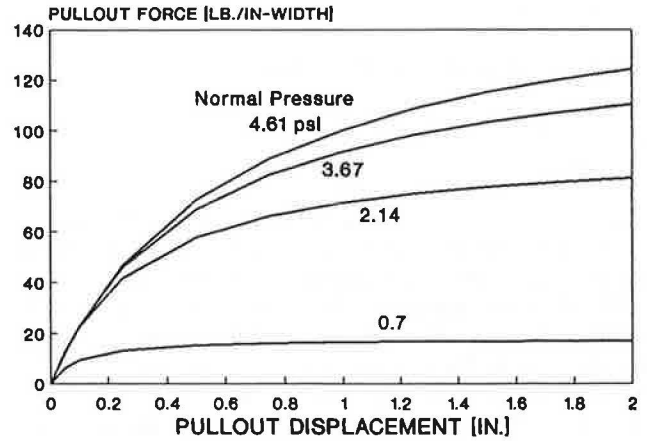

FIGURE 6 Results of pullout box test with geogrid (Tensar UX1100) in sand.

mulation. The shear stiffness parameters, a and b, are changed until the predicted pullout characteristics match those shown in Figures 5 and 6, respectively. This approach, which is discussed in Yuan and Chua (*9*), seems complicated, but it is not difficult. The results serve to explain what actually occurs at soil-reinforcement interfaces. It can be seen from Figures 7 and 8 that the shear stiffness of the sand-geotextile interface reduces more rapidly than that of sand-geogrid interface with pullout displacement.

Summary

The nonlinear responses seen in Figures 5–8 suggest that soil-reinforcement interaction is more complicated than usually assumed and that the pullout behavior of reinforcing materials is not uniform through the entire embedded length. The finite

element approach is convenient for some to use, but it may be unavailable as well as too costly for practicing engineers. In view of this, it will be shown that the analytical solution proposed earlier can to a large extent model the "real" soil-reinforcement interface.

ANALYTICAL MODELING: EXAMPLE PROBLEM

For this problem, assume that pullout tests are performed and the results shown in Figure 3 (pullout force versus strain) and Figures 5 and 6 (pullout versus displacement for Geolon 200 and Tensar UX1100, respectively) are obtained. The axial stiffnesses for Geolon 200 and Tensar UX1100 can be estimated from Figure 3 and are found to be about 1,300 and 4,350 lb/in.-width, respectively. Consider the reinforcing materials to be buried horizontally under 4 ft of sand at about 2 psi of vertical pressure. Referring to Figures 6 and 7, at some nonzero pullout displacement (say 0.05 in. to avoid the initial slope, which is reasonable because some movement will always occur), the slopes of the curves for a 2-psi normal pressure are 3 and 80 lb/in.-width for Geolon 200 and Tensar UX110, respectively. These slopes are the shear stiffnesses for the two reinforcing materials in that particular sand. Although the finite element approach of determining the shear stiffnesses is more accurate, this method of estimating the stiffness values is more convenient. It will also be an improvement over the assumption that the shear stress distribution is always uniform. These stiffness values will be used in the following discussions.

Pullout Displacements

Figure 9 shows curves of pullout displacements versus distance from the maximum tension line for the geotextile and geogrid under pullout forces of 2, 5, and 10 lb/in.-width. It can be seen that for the geogrid, very little displacement occurs beyond 2 ft from the maximum tension line. The length of the geotextile that is actually resisting the pullout can be seen to be only about 7 ft. This implies that even if the embedded reinforcement length is 40 ft beyond the maximum tension line, most of the material will be redundant. Unfortunately, this is often ignored and the state of the practice continues to assume that the entire embedded length is effective in resisting pullout.

The pullout resistance (P) is also seen to increase with an increasing pullout displacement (u), and this is consistent with pullout test results. Figure 9 shows this. This suggests that for an earth reinforcement to work, lateral movement is inevitable.

Reinforcement Tension

Figure 10 shows the distribution of the tensile force in the reinforcement along the length of the reinforcement for the geotextile and the geogrid at various pullout force levels. Again it can be seen that the tensile force in the reinforcement reduced very rapidly with distance from the maximum tension line.

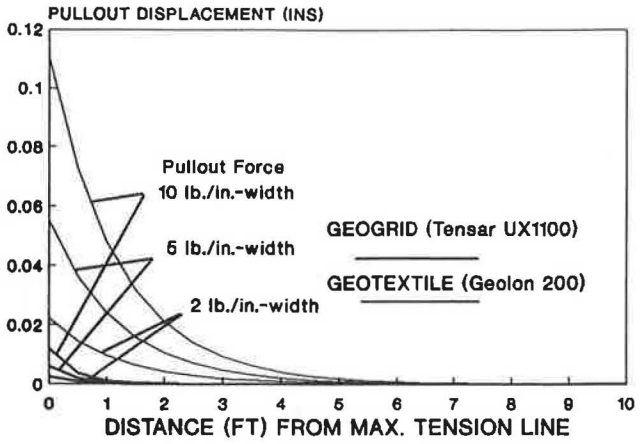

FIGURE 9 Computed pullout displacements along a long reinforcement (normal pressure 2 psi or 4 ft of sand).

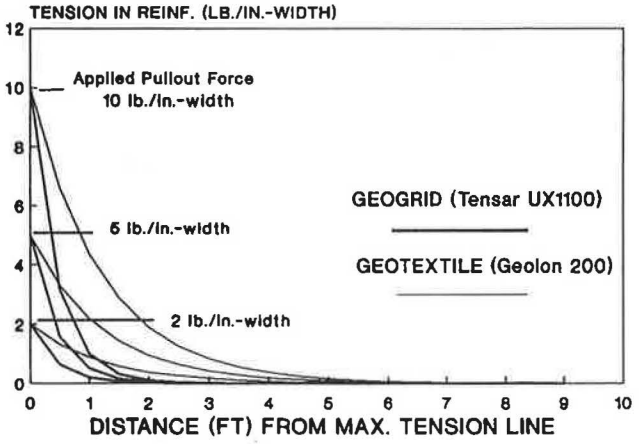

FIGURE 10 Computed tension along a long reinforcement (normal pressure 2 psi or 4 ft of sand).

Shear Stress Distribution

Figure 11 shows the shear stress distributions for the two reinforcing materials at different pullout force levels. The stress level reduces more rapidly in the stiffer reinforcement (Tensar UX1100) than in the geotextile.

Reinforcement Length

Figures 12–14 show the results obtained using the proposed solution for a 12-in.-long reinforcement. It can be seen from Figure 12 that the whole geotextile is being pulled about 0.13 in. through the soil when a 10 lb/in.-width pullout force is applied. The geogrid is seen to be holding fast to the soil. Figure 13 shows that both reinforcement types are completely in tension. The tension at the free end is zero, which is consistent with the principle of equilibrium because no tension

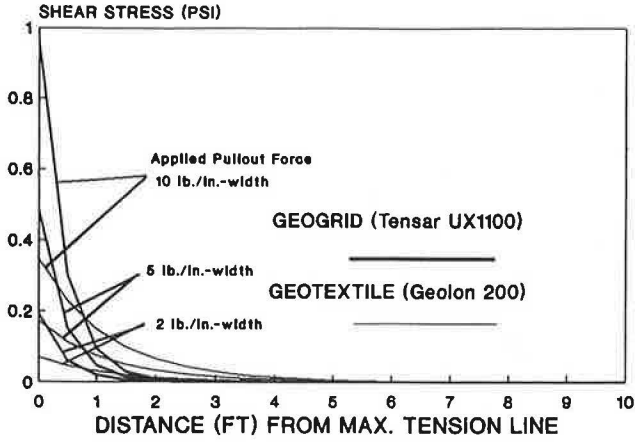

FIGURE 11 Computed shear stresses along a long reinforcement (normal pressure 2 psi or 4 ft of sand).

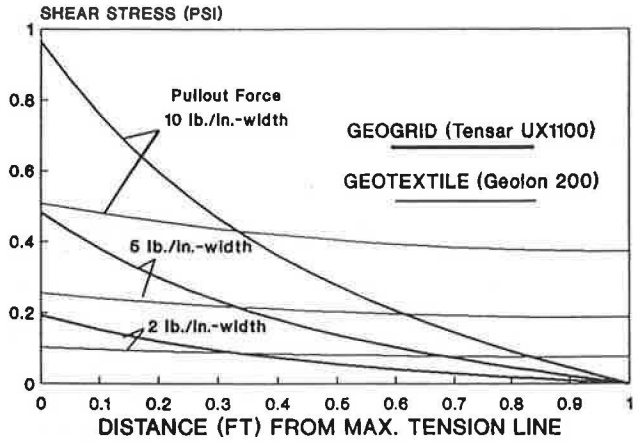

FIGURE 14 Computed shear stresses along a short reinforcement (normal pressure 2 psi or 4 ft of sand).

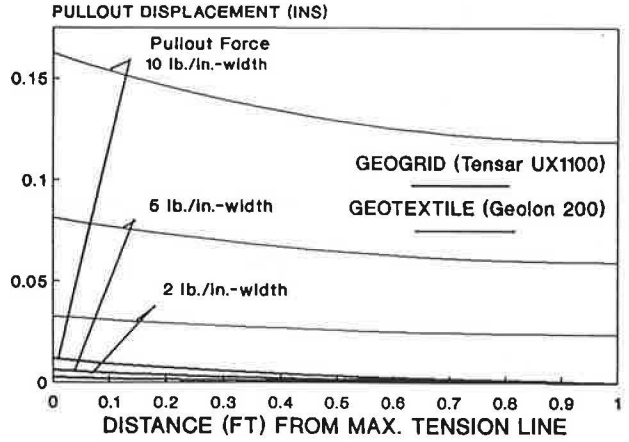

FIGURE 12 Computed pullout displacements along a short reinforcement (normal pressure 2 psi or 4 ft of sand).

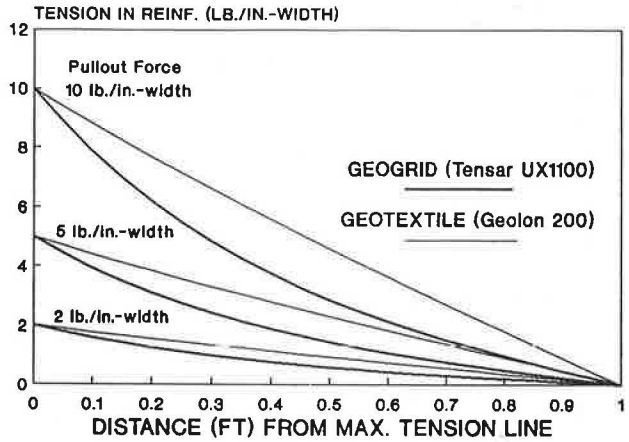

FIGURE 13 Computed tension along a short reinforcement (normal pressure 2 psi or 4 ft of sand).

can be derived from the soil. It is interesting to note in Figure 14 that the shear stresses at the free ends of the geotextiles are not zeros whereas those in the geogrid are.

It can be seen that the reinforcement length is an important consideration in determining the available pullout resistance. The pullout forces assumed here are relatively small. The force levels in the field will be much larger. The increase in vertical pressure will also give a stiffer shearing interface, which will cause the effective length of the reinforcement to increase.

CONCLUSIONS AND RECOMMENDATIONS

A closed-form solution for describing the pullout behavior of reinforcements in soils is presented here. It is shown that the pullout resistance (P) is an explicit function of four variables: pullout displacement (u), interface shear stiffness (k_s), reinforcement stiffness (k_a), and reinforcement length (L). The characteristics of the axial and shear stiffnesses are discussed. The proposed solution has practical merits that can be seen from the following recommendations for implementation.

1. The current design methods for reinforced earth walls and reinforced earth slopes do not consider pullout to be directly affected by reinforcement length. It seems that this factor can be easily incorporated into the current design practice if a minimum reinforcement length is specified on the basis of the axial and shear stiffnesses and the anticipated pullout force level. In recognizing that the effective length varies as a function of pullout, it may be possible to eliminate the otherwise redundant materials beyond the effective zone and be more cost-effective. Conversely, the solution can also be used to determine whether an available embedded length is adequate.

2. The shear stress at the soil reinforcement interface and the tensile stress in the reinforcement predicted by the analytical solution for the field condition can be compared with pullout test results to determine if slippage will occur at the

interface for that particular length of reinforcement. Because the length is included in the solution and shear stresses are correctly described as being nonuniform, the question as to whether the longitudinal dimension of any pullout box will affect laboratory pullout properties will not arise.

3. The pullout characteristics are affected by the ratio between the axial and the shear stiffness, so it may be possible to match reinforcement stiffnesses with different types of soil to optimize the design. It can be shown using the proposed solution that the tensile stresses in the reinforcement will be distributed more uniformly if the reinforcement stiffness is more compliant with the soil. This is an appreciable feature because the stresses will be less concentrated.

4. The proposed analytical model can be easily incorporated into existing slope stability analysis codes. This will give the added flexibility of allowing the pullout resistance to vary with depth as well as with reinforcement length. The axial stiffness and shear stiffness can be easily determined in the laboratory. Eventually, these determinations may be made from a data base.

5. It will also be possible to use the proposed solution to estimate the maximum pullout force at different reinforcement levels from observed lateral movement of a reinforced earth structure. This can provide a useful indication of the critical condition of any in-place reinforced earth structure.

REFERENCES

1. F. Schlosser and V. Elias. Friction in Reinforced Earth. *Proc., ASCE National Convention*, Pittsburgh, Pa., April 1978, pp. 735–763.
2. R. W. Lentz and J. N. Patt. Pull-Out Resistance of Geogrids in Sand. In *Transportation Research Record 1188*, TRB, National Research Council, Washington, D.C., 1988, pp. 48–55.
3. C. Bonczkiewicz, B. R. Christopher, and D. K. Atmatzidis. Evaluation of Soil-Reinforcement Interaction by Large-Scale Pull-Out Tests. In *Transportation Research Record 1188*, TRB, National Research Council, Washington, D.C., 1988, pp. 1–18.
4. R. K. Rowe, S. K. Ho, and D. G. Fisher. Determination of Soil-Geotextile Interface Shear Strength Properties. *Proc., 2nd Canadian Symposium on Geotextiles*, 1985, pp. 25–34.
5. A. Collios, P. Delmas, J. P. Gourc, and J. P. Giroud. Experiments on Soil Reinforcement with Geotextiles. *Proc., ASCE National Convention*, Portland, Oreg., 1980, pp. 53–73.
6. R. D. Holtz. Laboratory Studies of Reinforced Earth Using a Woven Polyester Fabric. *International Conference on the Use of Fabrics in Geotechnics*, Paris, France, 1977, pp. 149–154.
7. M. H. Vidal. The Development and Future of Reinforced Earth. *Proc., ASCE National Convention*, Pittsburgh, Pa., April 1978, pp. 1–61.
8. J. B. Carney. *A Test Chamber for the Determination of the Pullout Resistance of Soil Reinforcing Elements*. Report CE-76 (86) NMSHD-000757. Department of Civil Engineering, University of New Mexico, Albuquerque, March 1986.
9. Z. Yuan and K. M. Chua. Numerical Evaluation of the Pullout Box Method of Studying Soil-Reinforcement Interactions. In *Transportation Research Record 1278*, TRB, National Research Council, Washington, D.C., 1990, pp. 116–124.

Publication of this paper sponsored by Committee on Geosynthetics.